IOP Publishing Journal of Physics: Condensed Matter
J. Phys.: Condens. Matter **32** (2020) 275702 (6pp) https://doi.org/10.1088/1361-648X/ab7e5d

# Effects of vacancy defects on the mechanical properties in neutron irradiated Czochralski silicon

**Shangjie Jin[1], Peng Wang[1], Yazhou Qin[1], Can Cui[1,3], Deren Yang[2] and Xuegong Yu[2,3]**

[1] Key Laboratory of Optical Field Manipulation of Zhejiang Province, Department of Physics, Zhejiang Sci-Tech University, Hangzhou 310018, People's Republic of China
[2] State Key Lab of Silicon Materials, School of Materials Science and Engineering, Zhejiang University, Hangzhou 310027, People's Republic of China

E-mail: cancui@zstu.edu.cn and yuxuegong@zju.edu.cn

Received 24 July 2019, revised 21 February 2020
Accepted for publication 10 March 2020
Published 9 April 2020

**Abstract**

We have investigated the mechanical properties of neutron irradiated Czochralski (NICZ) silicon using nanoindentations combined with micro-Raman spectroscopy. It is found that NICZ silicon shows higher hardness (∼13% higher) than non-irradiated silicon, with a slightly lower Young's modulus. When the samples were subjected to isochronal anneals in the temperature range of 250 °C–650 °C, the hardness of NICZ silicon gradually decreases as the temperature increases and it is finally comparable to that of the non-irradiated silicon. The vacancies and vacancy–oxygen defects induced by neutron irradiation in NICZ silicon annihilate or transform into more complex defects during the annealing processes. It suggests that the vacancy defects play a role in the evolution of hardness, which promote phase transition from the Si-I phase to the stiffer Si-II phase in NICZ silicon during indentation. In addition, the irradiation induced vacancy defects could lead to the lower Young's modulus.

Keywords: Czochralski silicon, neutron irradiation, nanoindentation, hardness, vacancy defects

(Some figures may appear in colour only in the online journal)

## 1. Introduction

Czochralski (CZ) silicon is a dominating semiconductor material widely used in integrated circuits, solar cells and microelectromechanical systems (MEMS), both as a structural material for MEMS devices and as a substrate material for high compatibility with semiconductor processing equipment [1]. With the increasing diameter of silicon wafers used for microelectronics industry and the increasing requirements for silicon wafer processing, the mechanical performance of CZ silicon has drawn more and more attention. On the other hand, in order to reduce production costs, the thickness of silicon wafers used in solar cells is usually less than 200 μm, resulting in high fragment rate of silicon wafers during manufacture. Therefore, improving the mechanical strength of silicon wafers has become particularly vital as increasingly gravitational or thermal stresses might cause warpages or cracks of wafers in the manufacturing process [2, 3].

With the development of modern aviation industry and nuclear industry, silicon-based electronic components and integrated circuits are frequently used in irradiation environment. When silicon materials and silicon-based devices are bombarded with high energy particles, silicon atoms will deviate from their original positions and form point defects [4, 5], which affect the electrical and mechanical properties of silicon. Because the diffusion rate of interstitial silicon atoms is much higher than that of vacancies, interstitial silicon atoms tend to diffuse out of the surface, and a large number of vacancies remain in silicon [6]. The mobile vacancies easily interact with unavoidable oxygen impurities in CZ silicon and form

[3] Author to whom any correspondence should be addressed.

 

vacancy oxygen (VO) complex [7]. In the subsequent thermal treatment, VO complex prefers to trap the mobile vacancies or interstitial oxygen, forming $V_mO_n$ complexes such as $V_2O$, $VO_2$ and $VO_3$ [8]. The electrical properties of such V–O complexes in silicon have been extensively studied for years [9–11]. However, the effect of vacancy defects (mostly V–O complexes) on the mechanical properties of silicon has not been fully understood.

As we know, a number of studies have investigated the impacts of external impurities on the mechanical strength of CZ silicon [12–16]. Chen *et al* [13] have reported that germanium doping can block the mobilization of dislocations in CZ silicon, since the germanium-related complexes facilitate the generation of small and high density oxygen precipitates. Yang *et al* [14, 15] have reported that nitrogen doping can increase the activation energy of the dislocation motion, thus enhances the mechanical strength of CZ silicon. In addition, other impurities such as carbon and nickel have been implanted into silicon to improve the mechanical strength of silicon due to the increased bond energy between the impurities and silicon atoms [16].

In this work, neutron irradiation is carried out on CZ silicon to form point defects and then the mechanical properties of irradiated silicon have been investigated by means of nanoindentation measurements. The evolutions of V–O complexes in NICZ silicon during annealing have been characterized by Fourier transform infrared spectroscopy (FTIR) measurements. Micro-Raman spectroscopy measurements are used for phase transform analysis. The underlying mechanisms also have been discussed.

## 2. Experimental

The n-type, (100) oriented 4 inch CZ silicon wafers with a thickness of 2 mm were used in this study. The resistivity is $\sim$10 Ω·cm, measured by the four probe method, and the interstitial oxygen concentration is $9.3 \times 10^{17}$ cm$^{-3}$, determined by the FTIR technique at room temperature (RT) with a calibration coefficient of $3.14 \times 10^{17}$ cm$^{-2}$. The wafers were cutted into 20 mm × 20 mm pieces, and then they were divided into two groups. One was subjected to neutron irradiation in a fast neutron reactor at RT with a dose of $5 \times 10^{17}$ cm$^{-2}$, while the another was conventional CZ silicon as a reference. After irradiation, all the samples were subjected to chemical mechanical polishing, followed by standard RCA cleaning and dipping into the diluted HF solution for 3 min to remove the native oxide from the silicon surfaces. Then, the irradiated samples were isochronally annealed in argon atmosphere in the temperature range of 250 °C–650 °C for 20 min. The evolutions of V–O complexes in the samples during the annealing processes were monitored by FTIR at RT.

Nanoindentation tests were carried out at RT using a nanoindenter (Nanoindenter G200, USA) equipped with a Berkovich diamond indenter. A maximum load $P_{max}$ of 10 mN was performed with the holding time of 30 s to minimize the time-dependent plastic effect, and the constant loading/unloading rate was 0.05 mN s$^{-1}$. In this measurement, the ⟨110⟩ direction of the samples was parallel to one face of the indenter. Each sample was indented at seven points to check reproducibility of the data. The phase transitions induced by indentation in the specimens were investigated using a micro-Raman spectroscopy (Renishaw, UK) with the excitation wavelength of 532 nm from an $Ar^+$ laser. The laser beam size was about 4 μm, and the laser power was 20 mW with an integration time of 10 s. Raman spectra were acquired on indentations, which were produced by a Vickers microindenter with a load of 10 g and a loading/unloading rate of 30 mN s$^{-1}$.

## 3. Results and discussion

Figure 1 shows two typical selected load–displacement ($P$–$h$) curves for the CZ and NICZ silicon specimens, respectively. As can be seen, the CZ and NICZ silicon show similar $P$–$h$ curves with continuous loading/unloading segments, associated with pop-out events in both specimens during the unloading process. Jang *et al* [17] demonstrated that no cracks were formed when the indentation $P_{max}$ was lower than 80 mN. Hence, there are no cracks introduced in the indentation region and dislocations are difficult to generate when the $P_{max}$ is 10 mN in our investigation. The samples only undergo elastic and plastic deformation during loading [18]. The plastic deformation is dominated by the phase transition from the cubic diamond phase (Si-I) to the metallic β-Sn structure phase (Si-II) during the loading process [19]. The unloading curves depend on loading/unloading rate and $P_{max}$. In general, slower loading/unloading rate and higher $P_{max}$ result in the Si-II phase transforming to body centered cubic phase (Si-III) and rhombohedral structure phase (Si-XII), consequently pop-out in the unloading segment appears. While at faster rates and lower loads, the Si-II phase can further transform to amorphous phase (a-Si), in this case, elbows are often observed [20]. For the $P_{max}$ of 10 mN and unloading rate of 0.05 mN s$^{-1}$, pop-out effects generally occur in CZ silicon [17, 20]. In this work, pop-out effects are also observed in both samples, which coincide with the results reported before. Moreover, it can be clearly seen from figure 1 that the maximum indentation displacement in the CZ silicon is about 16 nm deeper than that in NICZ silicon, which means that the hardness of the NICZ silicon is larger than that of the CZ silicon. Therefore, we speculate that neutron irradiation has an influence on the mechanical properties of CZ silicon.

The values of hardness can be determined from the following formula,

$$H = \frac{P_{max}}{A} \tag{1}$$

where $H$ is the hardness, $P_{max}$ is the maximum load and $A$ is the projected area of contact at maximum load.

The Young's modulus of the specimens can be calculated using the Oliver–Pharr method [21] through the following formula,

$$\frac{1}{E_r} = \frac{1-\nu^2}{E} + \frac{1-\nu_i^2}{E_i} \tag{2}$$

where $E_r$ is relative modulus, which can be extracted from the unloading–displacement data. $E$ and $\nu$ are the Young's modulus and Poisson's ratio for the specimen, $E_i$ and $\nu_i$ are

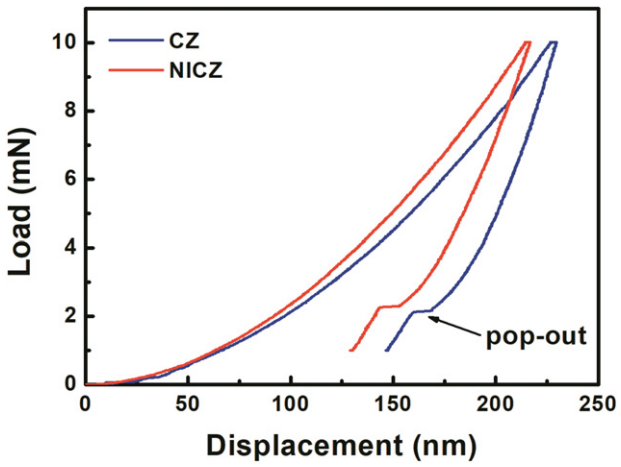


**Figure 1.** Nanoindentation load–displacement ($P$–$h$) curves of the CZ and NICZ silicon with characteristic event ('pop-out') in the unloading segment, obtained at a constant loading/unloading rate of 0.05 mN $s^{-1}$ and maximum load $P_{max}$ of 10 mN.

those for the indenter, respectively. For the diamond indenter, $E_i = 1141$ GPa, $\nu_i = 0.07$, and for silicon, $\nu = 0.3$ [21].

The hardness of the CZ and NICZ silicon samples are calculated to be $10.29 \pm 0.29$ GPa and $11.58 \pm 0.24$ GPa, respectively, as illustrated in figure 2. Note that the hardness of the CZ silicon is consistent with the reported values [22]. The Young's modulus of the CZ and NICZ silicon samples are calculated to be $190.69 \pm 6.03$ GPa and $185.52 \pm 6.43$ GPa, respectively. The results demonstrate that the hardness of NICZ samples obviously increases after neutron irradiation, by a percentage of ~13%. Meanwhile, the Young's modulus of NICZ samples slightly decreases.

The Young's modulus is a result of the interatomic forces between the constituent atoms [1]. Under the condition of neutron irradiation, a high concentration of point defects are generated in silicon [5]. Previous reports have demonstrated that Young's modulus of silicon decreases with increasing point defect concentration based on theoretical calculation, and moreover, its changes are confined to a surprisingly small range [23, 24]. The simulation result is in good agreement with the slightly reduced Young's modulus in our experimental results, and we thus believe that it is mainly attributed to the vacancy defects caused by irradiation which reduce the bonding forces between silicon atoms to some extent. On the other hand, the hardness of the NICZ samples significantly increases compared with the CZ samples. It is now generally accepted that the overall hardness is determined by the phase transformations in silicon [25]. As the phase transition often occurs in the process of nanoindentation [26, 27], it is thus considered that the phase transition may be the reason for the increase in hardness after neutron irradiation. However, the nanoindentation region is too small to measure the silicon phase transition directly by means of micro-Raman technique. Microindentation induces similar phase transition behaviors with nanoindentation during loading [28], which can be applied to analyze the phase transformation and hardness changes in CZ and NICZ silicon as follows.

Figure 3(a) shows the Raman spectra for undeformed region of CZ and NICZ silicon. Both specimens exhibit a sharp peak at 520 $cm^{-1}$ corresponding to the Si-I phase in the Raman spectra [29]. The intensity of Si-I phase of NICZ silicon is a little smaller than that of CZ silicon. The irradiation-induced reduction of crystalline phase intensity was also observed in previous work in neutron irradiated silicon [30]. Note that the specimens have undergone polishing process, thus the possible amorphization close to the surface cannot be observed. As can be seen in figure 3(b), with loading of microindentation, the characteristic Raman peaks of the Si-I phase shift to 522 $cm^{-1}$ because of the residual compressive stresses. Besides, there appear three broad peaks around 160, 300, 470 $cm^{-1}$ corresponding to the characteristic Raman peaks of the a-Si phase [31–33]. More importantly, the peaks of the a-Si phase in the NICZ silicon are stronger than those in the CZ silicon, while the Si-I phase peak of the former is much weaker than the latter.

The phase transition often occurs during microindentation in the form of Si-I → Si-II → a-Si [18, 27]. Youssef *et al* [26] have reported that the transformation of Si-I phase to Si-II phase may be the cause of variation in the hardness of the CZ silicon. The Si-II phase generated during the indentation test is a metastable phase, which converts into the a-Si phase very quickly when the indenter is withdrawn. Though the existence of Si-II phase cannot be directly observed, the relative content of Si-II phase can be estimated by analyzing the Raman peak of a-Si phase. The intensity of the a-Si peak at 470 $cm^{-1}$ of the NICZ silicon is much higher than that of the CZ silicon, indicating the formation of more a-Si phase in the NICZ silicon after indentation. Therefore, it is inferred that more Si-II phase is generated in the NICZ silicon due to the transitions of Si-I → Si-II → a-Si. Si-II phase has a higher hardness than Si-I phase [28], therefore the NICZ silicon show a higher hardness that the CZ silicon.

The neutron irradiation can introduce a large number of vacancies, which will further transform into V–O complexes in CZ silicon during subsequent thermal treatment [4]. The generation of vacancy defects causes lattice distortion and higher free energy around the vacancy defects, leading to an increasing driving force of phase transformation [34, 35]. This may promote the nucleation of a high-pressure phase, i.e., facilitate the phase transition from the Si-I phase to the Si-II phase in the NICZ silicon during indentation, thereby enhances the hardness of silicon. Previous studies have shown that the introduction of impurities affect the phase transformation behavior of silicon. Zeng *et al* [31] have confirmed that germanium doping promotes phase transition from the Si-I phase to the stiffer Si-II phase, thereby increases the hardness of CZ silicon under indentation. In order to verify the above conjecture, isochronal anneals were further performed to modulate the concentration of vacancy defects in NICZ silicon, followed by the nanoindentation tests to obtain the hardness of the NICZ silicon.

Figure 4 shows FTIR spectra for NICZ silicon after isochronal anneals in the temperature range of 250 °C–650 °C for 20 min. FTIR is the most powerful characterization technique to investigate the vacancy defects in silicon, and the

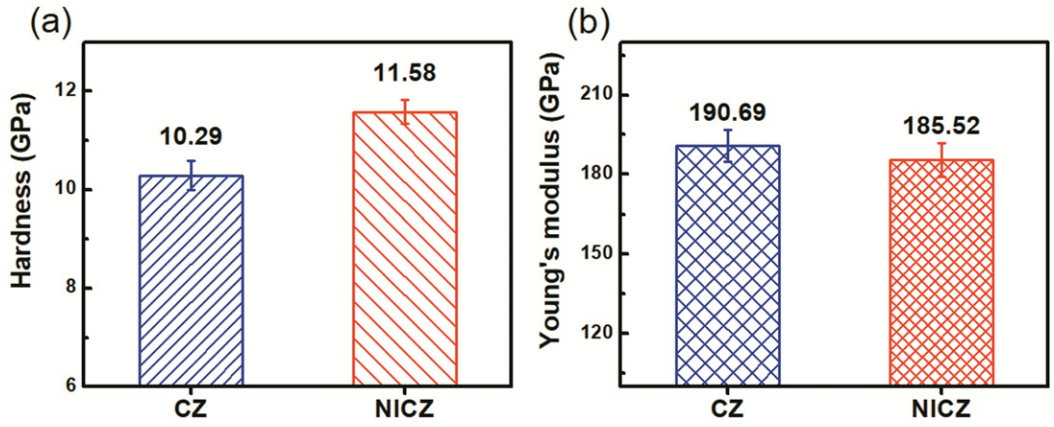


**Figure 2.** Histograms of (a) hardness and (b) Young's modulus comparisons for CZ and NICZ silicon.

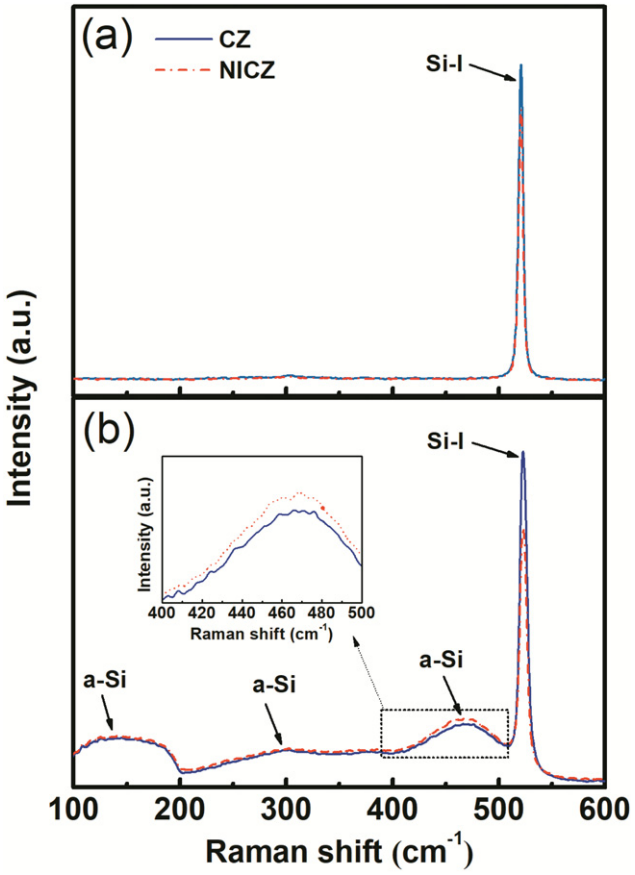


**Figure 3.** Raman spectra taken from CZ and NICZ silicon on (a) pristine material outside the impression and (b) Vickers impressions. The indentations were produced by a Vickers microindenter with a load of 10 g and a loading/unloading rate of 30 mN $s^{-1}$.

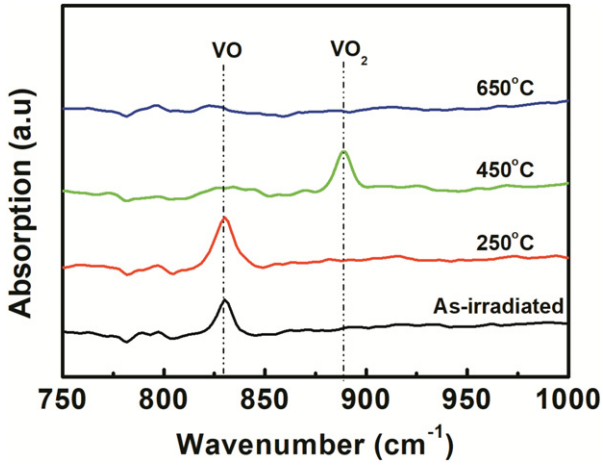


**Figure 4.** Room temperature FTIR absorption spectra of the NICZ silicon subjected to isochronal anneals in argon atmosphere in the temperature range of 250 °C–650 °C for 20 min.

IR absorption bands related to $V_mO_n$ complexes are usually observed in the range of 800–1100 $cm^{-1}$ [36–39]. The 830 $cm^{-1}$ band originates from VO complex, while the 889 $cm^{-1}$ band corresponds to the $VO_2$ complex [36]. These V–O complexes are formed by interstitial oxygen ($O_i$) capturing the mobile vacancies caused by neutron irradiation [37]. It can be obviously seen from figure 4 that only the VO complex peak appears in the as-irradiated sample. After annealing at 250 °C, the intensity of VO complex continues to increase as a result of capture of more vacancies by $O_i$. With increasing temperature, the VO complex is decomposed into individual vacancy and $O_i$ by the reaction of VO → V + $O_i$. Simultaneously, the $VO_2$ complex is formed by the reaction of VO + $O_i$ → $VO_2$ [40]. Therefore, after annealing at 450 °C, the VO complex band completely vanishes, meanwhile the $VO_2$ complex is observed in the NICZ samples. When the annealing temperature increases up to 650 °C, both the peaks of VO and $VO_2$ complexes disappear. It is believed that, the VO and $VO_2$ complexes will form more complicated $V_mO_n$ complexes [41], while the rest part of vacancies could recombine with interstitial silicon atoms or diffuse out of the silicon surface, thereby reducing the amount of vacancies in silicon.

Figure 5 shows the hardness variation of the NICZ silicon after isochronal anneals. It can be seen that, the hardness of the NICZ silicon decreases gradually from 11.58 ± 0.24 GPa to 10.06 ± 0.28 GPa with increasing annealing temperature from 250 to 650 °C. In other words, the hardness of the samples decreases with the decrease of vacancy defect concentration. Note that the hardness almost recovers to the original value without irradiation after annealing at 650 °C. It is evident that

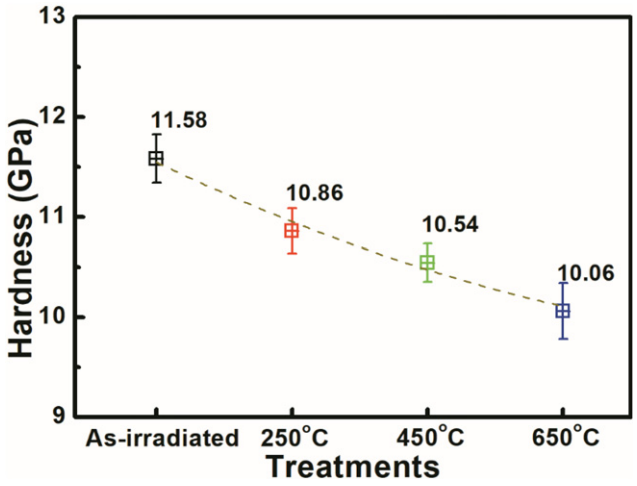


**Figure 5.** Variation of the hardness of the NICZ silicon as a function of the annealing temperature. The samples subjected to isochronal anneals in argon atmosphere in the temperature range of 250 °C–650 °C for 20 min. Each error bar represents the maximum deviation.

with the reduction of the vacancy concentration during annealing processes, the silicon lattice is almost restored to the original arrangement, which may mitigate the phase transition from Si-I phase to the stiffer Si-II phase under indentation and thus result in the reduction of the hardness of the NICZ silicon.

## 4. Conclusion

We have studied the effects of vacancy defects on the mechanical properties in NICZ silicon. The NICZ silicon has higher hardness (∼13% higher) in average compared with CZ silicon. It is found that the vacancy defects induced by neutron irradiation, promote the phase transition from Si-I phase to the stiffer Si-II phase, resulting in an improvement in the hardness of the NICZ silicon. After isochronal anneals in the temperature range of 250 °C–650 °C, the concentration of vacancies decreases in the forms of annihilation and transforming into more complex defects, leading to a decrease of the hardness of NICZ silicon to the original level. In addition, the NICZ silicon has slightly lower Young's modulus in average, which could be due to the reduced bonding forces between silicon atoms induced by the vacancy defects.

## Acknowledgments

This project is supported by National Natural Science Foundation of China (No. 61604131, 51532007, 61974129), Science Challenge Project (No. TZ2016003-1), Natural Science Foundation of Zhejiang Province (No. LY19F040009, No. LY17F040005), Scientific Research Foundation of Zhejiang Sci-Tech University (No. 16062067-Y).

## ORCID iDs

Can Cui https://orcid.org/0000-0002-8429-5875
Xuegong Yu https://orcid.org/0000-0002-0354-8501

## References

[1] Hopcroft M A, Nix W D and Kenny T W 2010 What is the Young's modulus of silicon? *J. Microelectromech. Syst.* **19** 229–38
[2] Fischer A and Kissinger G 2007 Load induced stresses and plastic deformation in 450 mm silicon wafers *Appl. Phys. Lett.* **91** 111911
[3] Hu S 1969 Temperature distribution and stresses in circular wafers in a row during radiative cooling *J. Appl. Phys.* **40** 4413–23
[4] Chroneos A, Sgourou E, Londos C and Schwingenschlögl U 2015 Oxygen defect processes in silicon and silicon germanium *Appl Phys. Rev.* **2** 021306
[5] Kraitchinskii A, Kolosiuk A, Kras'ko M, Neimash V, Voitovych V, Makara V, Petrunya R and Putselyk S 2011 Vacancy generation in silicon in the temperature range 100–633 K under electron irradiation *Radiat. Eff. Defects Solids* **166** 445–50
[6] Falster R, Voronkov V and Quast F 2000 On the properties of the intrinsic point defects in silicon: a perspective from crystal growth and wafer processing *Phys. Status Solidi* B **222** 219–44
[7] Mikelsen M, Bleka J, Christensen J, Monakhov E, Svensson B, Härkönen J and Avset B 2007 Annealing of the divacancy-oxygen and vacancy-oxygen complexes in silicon *Phys. Rev.* B **75** 155202
[8] Alfieri G, Monakhov E, Avset B and Svensson B 2003 Evidence for identification of the divacancy-oxygen center in Si *Phys. Rev.* B **68** 233202
[9] Alfieri G, Monakhov E V, Avset B S and Svensson B G 2003 Evidence for identification of the divacancy-oxygen center in Si *Phys. Rev.* B **68** 233202
[10] Mikelsen M, Bleka J H, Christensen J S, Monakhov E V, Svensson B G, Härkönen J and Avset B S 2007 Annealing of the divacancy-oxygen and vacancy-oxygen complexes in silicon *Phys. Rev.* B **75** 155202
[11] Evans-Freeman J, Kan P and Abdelgader N 2002 High resolution deep level transient spectroscopy studies of the vacancy-oxygen and related defects in ion-implanted silicon *J. Appl. Phys.* **92** 3755–60
[12] Alpass C, Murphy J, Falster R and Wilshaw P 2009 Nitrogen diffusion and interaction with dislocations in single-crystal silicon *J. Appl. Phys.* **105** 013519
[13] Chen J, Yang D, Ma X, Zeng Z, Tian D, Li L, Que D and Gong L 2008 Influence of germanium doping on the mechanical strength of Czochralski silicon wafers *J. Appl. Phys.* **103** 123521
[14] Yang D R and Yu X 2004 Nitrogen in silicon *Defect Diffus. Forum* **230** 199–220
[15] Li D S, Yang D R and Que D L 1999 Effects of nitrogen on dislocations in silicon during heat treatment *Phys.* B **273–274** 553–6
[16] Xu Z H, Park Y B and Li X 2010 Nano/micro-mechanical and tribological characterization of Ar, C, N, and Ne ion-implanted Si *J. Mater. Res.* **25** 880–9
[17] Jang J I, Lance M, Wen S, Tsui T Y and Pharr G 2005 Indentation-induced phase transformations in silicon: influences of load, rate and indenter angle on the transformation behavior *Acta Mater.* **53** 1759–70
[18] Bradby J, Williams J, Wong-Leung J, Swain M V and Munroe P 2001 Mechanical deformation in silicon by micro-indentation *J. Mater. Res.* **16** 1500–7
[19] Zarudi I, Zou J and Zhang L 2003 Microstructures of phases in indented silicon: a high resolution characterization *Appl. Phys. Lett.* **82** 874–6
[20] Domnich V, Gogotsi Y and Dub S 2000 Effect of phase transformations on the shape of the unloading curve in the nanoindentation of silicon *Appl. Phys. Lett.* **76** 2214–6

[21] Oliver W C and Pharr G M 1992 An improved technique for determining hardness and elastic modulus using load and displacement sensing indentation experiments *J. Mater. Res.* **7** 1564–83
[22] Haberl B, Aji L B B, Williams J S and Bradby J E 2012 The indentation hardness of silicon measured by instrumented indentation: what does it mean? *J. Mater. Res.* **27** 3066–72
[23] Allred C L, Yuan X, Bazant M Z and Hobbs L W 2004 Elastic constants of defected and amorphous silicon with the environment-dependent interatomic potential *Phys. Rev.* B **70** 134113
[24] Li C X, Meng Q Y and Zhong K Y 2009 Atomistic study of the strength and elastic constants of perfect and defected silicon *Int. J. Mod. Phys.* B **23** 2365–71
[25] Vandeperre L J, Giuliani F, Lloyd S J and Clegg W J 2007 The hardness of silicon and germanium *Acta Mater.* **55** 6307–15
[26] Youssef K, Shi M, Radue C, Good E and Rozgonyi G 2013 Effect of oxygen and associated residual stresses on the mechanical properties of high growth rate Czochralski silicon *J. Appl. Phys.* **113** 133502
[27] Ge D, Domnich V and Gogotsi Y 2003 High-resolution transmission electron microscopy study of metastable silicon phases produced by nanoindentation *J. Appl. Phys.* **93** 2418–23
[28] Domnich V and Gogotsi Y 2002 Phase transformations in silicon under contact loading *Rev Adv. Mater. Sci.* **3** 1–36
[29] Merlin R, Pinczuk A and Weber W 2000 Overview of phonon Raman scattering in solids *Raman Scattering in Materials Science* (Berlin: Springer) pp 1–29
[30] Coeck M and Laermans C 2002 The search for tunnelling states in bulk silicon disordered by fast neutron irradiation *Defect Diffus. Forum* **200–202** 47–66
[31] Zeng Z, Wang L, Ma X, Qu S, Chen J, Liu Y and Yang D 2011 Improvement in the mechanical performance of Czochralski silicon under indentation by germanium doping *Scr. Mater.* **64** 832–5
[32] Wu K, Yan X and Chen M 2007 *In situ* Raman characterization of reversible phase transition in stress-induced amorphous silicon *Appl. Phys. Lett.* **91** 101903
[33] Haberl B, Liu A, Bradby J, Ruffell S, Williams J and Munroe P 2009 Structural characterization of pressure-induced amorphous silicon *Phys. Rev.* B **79** 155209
[34] Zarkevich N A, Chen H, Levitas V I and Johnson D D 2018 Lattice instability during solid-solid structural transformations under a general applied stress tensor: example of Si I-> Si II with metallization *Phys. Rev. Lett.* **121** 165701
[35] Javanbakht M and Levitas V I 2016 Phase field simulations of plastic strain-induced phase transformations under high pressure and large shear *Phys. Rev.* B **94** 214104
[36] Svensson B G and Lindstrom J L 1986 Kinetic-study of the 830 and 889 $cm^{-1}$ infrared bands during annealing of irradiated silicon *Phys. Rev.* B **34** 8709–17
[37] Yu X G, Chen L, Chen P and Yang D R 2012 Quantitative study of the evolution of oxygen and vacancy complexes in Czochralski silicon *Appl. Phys. Express* **5** 021302
[38] Ganagona N, Vines L, Monakhov E and Svensson B G 2014 Transformation of divacancies to divacancy-oxygen pairs in p-type Czochralski-silicon; mechanism of divacancy diffusion *J. Appl. Phys.* **115** 034514
[39] Hasegawa M, Tang Z, Nagai Y, Nonaka T and Nakamura K 2002 Positron lifetime and coincidence Doppler broadening study of vacancy-oxygen complexes in Si: experiments and first-principles calculations *Appl. Surf. Sci.* **194** 76–83
[40] Qin Y, Wang P, Jin S, Cui C, Yang D and Yu X 2019 Effects of nitrogen doping on vacancy-oxygen complexes in neutron irradiated Czochralski silicon *Mater. Sci. Semicond. Process.* **98** 65–9
[41] Cui C, Yang D, Ma X and Li M 2008 Oxygen precipitation in Czochralski silicon: Effect of ramped anneal from 300 to 750 °C *J. Appl. Phys.* **103** 064911